International Journal of Thermophysics, Vol. 27, No. 6, November 2006 (© 2006)
DOI: 10.1007/s10765-006-0072-z

On the Use of the Transient Hot-Strip Method for Measuring the Thermal Conductivity of High-Conducting Thin Bars[1]

M. Gustavsson,[2,3] H. Wang,[4] R. M. Trejo,[4] E. Lara-Curzio,[4] R. B. Dinwiddie,[4] and S. E. Gustafsson[5]

The thermal conductivity of thin, high-conducting ceramic bars—commonly used in mechanical tensile testing—is measured using a variant of the short transient hot-strip technique. As with similar contact transient methods, the influence from the thermal contact resistance between the sensor and the sample is accurately recorded and filtered out from the analysis—a specific advantage that enables sensitive measurements of the bulk properties of the sample material. The present concept requires sensors that are square in shape with one side having the same width as the bar to be studied. As long as this requirement is fulfilled, the particular size of the thin bar can be selected at will. This paper presents an application where the present technique is applied to study structural changes or degradation in reinforced carbon–carbon (RCC) bars exposed to thermal cycling. Simultaneously, tensile testing and monitoring of mass loss are conducted. The results indicate that the present approach may be utilized as a non-destructive quality control instrument to monitor local structural changes in RCC panels.

KEY WORDS: hot-strip; non-destructive testing; quality control; reinforced carbon–carbon; thermal conductivity; thermal degradation.

[1] Paper presented at the Seventeenth European Conference on Thermophysical Properties, September 5–8, 2005, Bratislava, Slovak Republic.

[2] CIT Foundation, Chalmers Science Park, SE-41288 Gothenburg, Sweden.
[3] To whom correspondence should be addressed. E-mail: Gustavsson@cit.chalmers.se
[4] Oak Ridge National Laboratory, Oak Ridge, Tennessee, U.S.A.
[5] Department of Physics, Chalmers University of Technology, SE-41296 Gothenburg, Sweden.

1. INTRODUCTION

The transient plane source (TPS) [1–8], the transient hot-strip (THS) [9–13], and the pulse transient hot-strip (PTHS) techniques [14–17] are used for measuring the thermal properties of materials, covering a wide range of materials and sample geometries.

A sensor in the shape of a strip, strip pattern, disk, or disk pattern is applied to a sample. It can be sandwiched either between two identical pieces of the sample—here referred to as a double-sided configuration—or applied to only one sample piece—here referred to as a single-sided configuration. The sensor is used simultaneously as a resistance heater and a resistance thermometer. Step-wise heating of the sensor is applied which results in a transient temperature increase of the near sample surroundings and the sensor itself. By recording the temperature rise of the sensor element, typically of the order of 1 K, the thermal transport properties of the sample can be accurately estimated.

The original analytical models used in fitting to experimental data assume infinite sample geometry, where the sensor is embedded in the sample. In practical experiments, the validity of this assumption is maintained by controlling the duration of the experiment in a way that only the first part of the transient response is considered for which the thermal profile development around the sensor has not yet reached the sample surface boundaries. In the following, the corresponding minimum distance between the sensor and the lateral sample surface boundary is referred to as the available probing depth.

For most homogeneous samples having medium or low thermal conductivity, a sample geometry of at least a couple of millimeters in thickness normally suffices for a straightforward experimental setup and measurement procedure. However, if the sample thickness is smaller, or the sample has a high thermal conductivity, the original approach may prove difficult since the measurement time is significantly reduced to a range, which may be difficult to attain with standard laboratory equipment.

This paper discusses the possibilities of extending the nominal measurement time considerably for high-thermal conductivity samples by adjusting the sample geometry configuration rather than by increasing the sample size. In particular, by utilizing thermal insulation, "mirroring" effects can be accomplished, which reduce the sample size considerably. When proposing a theoretical model to be used in data analysis for such a geometrical configuration, the available probing depth will not be limited by any of the mirroring surfaces. For instance, in Refs. [18] and [19]—discussing a modification referred to as the slab technique in the following—it is shown that thin sheets (of the order of 1 mm thickness) of

high thermal conductivity materials—such as Cu, Al, brass, and stainless steel—can efficiently be thermally insulated and measured with good accuracy. This arrangement applies to a theory where the available probing depth is defined by the minimum distance between the sensor and the lateral surface boundaries of the sides of the sheets (in the same plane as the sensor itself). In this way, the experimental time is extended from the range of milliseconds to several seconds. The reason this approach proved successful is that the loss of heat to the surrounding thermal insulation—through the mirroring surfaces—turns out to be negligible compared to the input of power needed to increase the temperature of the hot disk sensor.

A different type of mirroring was previously applied for high-thermal conductivity samples, making it possible to experimentally simulate the transient behavior of a much larger sensor and sample. With the short transient hot-strip (STHS) technique [20], a symmetric two-dimensional (2D) thermal profile in accordance with the basic THS theory is achieved by thermally insulating a thin cut-out cross section of the imagined sample, where symmetry boundaries in the original configuration can be replaced by mirroring surfaces. In this way, a small sample can be used to simulate a thermal conductivity experiment of a much larger sample. Consequently, the experimental time is prolonged while the sample is limited to a convenient size.

A combined STHS and slab approach is developed and utilized here for the study of the thermal conductivity of high-thermal conductivity sample bars of a well-defined geometry. By solving the thermal conductivity equation for this particular geometry, the theoretical time dependence of the temperature increase as a result of a step-wise heating can be established, cf. Section 2.

To test this technique in a practical application, the present approach is tested for the study of structural changes in high-thermal conductivity bar-shaped samples. In Section 4, an application is presented where changes in thermal conductivity of ceramic bars due to structural change is monitored. It is found that—in line with literature results suggesting the thermal conductivity is a sensitive indicator of the structural constitution of the sample [21]—the mass loss and degradation of mechanical properties of reinforced carbon–carbon (RCC), due to thermal cycling, can be monitored and correlated with corresponding changes in thermal conductivity. The structural changes caused by repeated thermal cycling are in this test case oxidation-induced mass loss and sub-surface damage (sub-surface oxidation, void formation, delamination, etc.).

2. THEORY

When performing thermal conductivity measurements with transient methods, it is often possible to design the experimental setup so that one can measure and eliminate the direct influence of any thermal contact resistance between the sensor probe and the surface of the solid sample material. An effective way is to set up the measurement so that the temperature response of the sensor, ΔT, is the sum of two clearly separable components—one component which is essentially constant [22], A, representing the total thermal contact resistance between the sensing material and the first solid surface of the sample, and the second component a transient component, $Bf(\tau_c)$, not influenced by any thermal contact resistance [5, 7, 22]:

$$\Delta T = A + Bf(\tau_c) \tag{1}$$

where $B = B\left(P_0/(\lambda_B l_1)\right)$, cf. Refs. [1, 6, 7], and [19]. In Eq. (1), the constant B incorporates the bulk thermal conductivity λ_B of the sample, the heating power P_0, and a characteristic length dimension l_1 of the probe, *e.g.*, strip length or disk radius. The dimensionless time function f is expressed in terms of the dimensionless time $\tau_c = \sqrt{(t - t_c)/\theta}$, where t is the real measurement time, t_c is a time correction, and $\theta = l_2^2/a$ represents the characteristic time of the measurement. The characteristic length scale l_2 represents the strip width or the disk radius, and a is the thermal diffusivity of the sample.

A large contacting area, typically the case for THS, PTHS, and TPS techniques—in contrast to the similar transient hot-wire (THW) technique—gives improved thermal contact between the sensor and the sample. This reduces the magnitude of component A. Also, a sensor with thin insulation reduces the heat capacity of the sensor itself, with additional improvements. To be more precise, one can show that the component A may vary slightly due to imperfect electronics as well as due to the heat capacity of the sensor itself [8]. To take into account the effects of a slightly varying component A, Eq. (1) may be reformulated into a corresponding model with a strictly constant A, as outlined in Ref. [8].

The time function f depends on the probe design and size, as well as the sample geometry. If the sample is assumed to be infinite in all directions—a common assumption for, e.g., THS, PTHS, TPS, and THW techniques—Eq. (1) remains valid in the time interval from the beginning of the transient to the instant in time, t_{max}, when the thermal penetration depth Δ_p reaches the nearest sample surface boundary. We can express

this time interval as (t_c, t_{max}), where

$$\Delta_p = 2\,(a t_{max})^{1/2} \tag{2}$$

represents the minimum distance from any part of the heating area of the sensor to the lateral boundary of the sample, i.e., the available probing depth.

Two issues limit the performance of this class of techniques. First, the measurement time: the sample and probe size selected may give large variations in the possible time interval, creating a problem if the maximum time t_{max} is very short. The second issue limiting the performance is the measurement sensitivity, which is governed by the selection of the probe and sample size configuration but also the measurement time; for instance, when using a hot-disk sensor, the optimal total measurement time t_{meas} should be selected within the interval $0.33 < t_{meas}/\theta < 1$, provided the available probing depth does not limit the measurement time, i.e., $t_{meas} < t_{max}$ [23].

From Eq. (2), it is obvious that high-thermal diffusivity samples or samples which have a small available probing depth Δ_p, result in very short maximum times t_{max}—which adversely influence measurement performance and make a measurement difficult to perform with standard laboratory multimeters, if t_{max} is shorter than, say, 0.5 s.

The average temperature response and time function for a double-sided 2D-slab THS configuration studied in this paper can be expressed as

$$\overline{\Delta T\,(\tau_c)} = A + \frac{P_0}{2\pi^{1/2} h \lambda_B} f\,(\tau_c) \tag{3}$$

where

$$f\,(\tau) = \int_0^{\tau} \left\{1 - \operatorname{erfc}\left(\frac{1}{\sigma}\right) - \frac{\sigma}{\pi^{1/2}}\left[1 - \exp\left(-\frac{1}{\sigma^2}\right)\right]\right\} \times \left\{1 + 2\sum_{n=1}^{\infty} \exp\left[-\left(\frac{n}{\sigma}\right)^2 \left(\frac{z}{d}\right)^2\right]\right\} d\sigma. \tag{4}$$

Here, z is the thickness of a sample (bar thickness), $2d$ is the strip width, and $2h$ is the strip length. To derive Eq. (4), the method of images has been applied. The slab STHS configuration in Figs. 1 and 2 has a strip length $2h$ equal to the bar width. The strip width $2d$ is equal to the length of the strip along the bar-length direction.

Function $f(\tau)$ in Eq. (4) describes a situation where the sample has a limited thickness perpendicular to the hot-strip sensor plane, while the

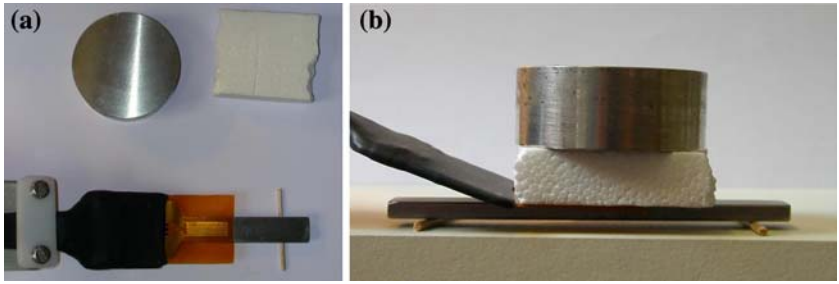

Fig. 1. (a) Single-sided setup and (b) centered strip sensor.

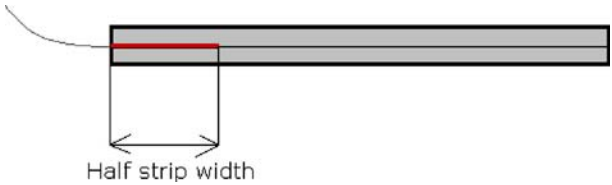

Fig. 2. Double-sided setup.

sample is considered infinite in the plane of the sensor. Equations (3) and (4) are identical to the expressions derived in Ref. [9] with the exception of the factor $2\sum_{n=1}^{\infty}\exp\left[-\left(n^2/\sigma^2\right)\left(z^2/d^2\right)\right]$. It is obvious that if z tends to infinity, one obtains the same function as that used in the THS method, where the sample is considered infinite in all directions.

In Fig. 1, we note that the single-sided configuration assumes a perfect mirroring—the symmetry boundary being the plane of the sensor—which requires us to assume a doubled output of heating power P_0 when analyzing data.

3. EXPERIMENTAL ARRANGEMENTS

A measurement system incorporating a bridge circuit with automatic compensation for lead resistances, a power supply and digital multimeter, as well as a data analysis module (supplied by Hot Disk Inc.) was used in this study.

A slab-based STHS configuration is obtained by cutting the samples into a shape that directly resembles a bar, cf. Figs. 1a and 1b, and insulating all sides. A double-sided setup may also be obtained in a similar way, cf. Fig. 2. The sensor can be placed in the center of the sample as in Figs. 1a and 1b or at one side of the configuration. In the latter case—where the sensor has been placed at the short end of the bar, cf. Fig. 2—an

additional mirrored surface appears at the short end of the bar (assuming a new symmetry boundary). In effect, if introducing a symmetry boundary at the short end of the bar, the transient response behavior will in effect behave as if the strip width has doubled (where the short end of the bar will represent the "center" of the strip width). The theoretical model to be used in accordance with the principal model in Eq. (1) will in this case require an adjustment of parameter d in the time function f, cf. Eq. (4), and an adjustment of parameter l_2 in θ, compensating for the introduction of this new symmetry boundary. In addition, the assumed output of power P_0 must also be doubled. Reference [20] describes this procedure in detail.

4. INFLUENCE FROM THERMAL TREATMENT ON CERAMIC BARS

A RCC composite consists of a carbon fiber/matrix composite (for rigidity and strength), a silicon carbide fiber/matrix conversion coating for high-temperature oxide protection, and tetraethyl orthosilicate (TEOS) impregnation and a sodium silicate sealant for additional oxidation protection.

Three bar-shaped samples were prepared—2D C/C composites coated with SiC which were synthesized by pack cementation—in order to investigate the relationship between thermal conductivity, mass loss, and strength properties when subjected to thermal cycling. Repeated thermal cycling of the three samples was conducted—between 20°C (293 K) and 800°C (1073 K), with a 15-min hold at 800°C—and correlated with changes in mass, thermal conductivity, and mechanical strength.

The dimensions of the bars are: 103.6 mm length, 12.73 mm width, and 4.60 mm thickness, cf. Fig. 3. The mass loss and thermal conductivity were tested after 0, 1, 3, 5, 7, 10, and 15 cycles. The results on tensile testing and degradation in mechanical strength due to repeated thermal cycling—which has been found to correlate well with the decrease in thermal conductivity—is presented elsewhere (in preparation).

Measurements were conducted at room temperature, with a sensor placement at the end of the bar following the configuration depicted in Fig. 2 but only using one sample, i.e., a single-sided configuration with Styrofoam insulation on the other side (cf. Fig. 1b). For each bar, thermal conductivity measurements were conducted at both ends—referred to as the A and B positions. Figure 4 shows the thermal conductivity results based on averaging of five measurements. Identical experimental parameter settings (heating power, measurement time) and data point selections for

Fig. 3. Ceramic bars.

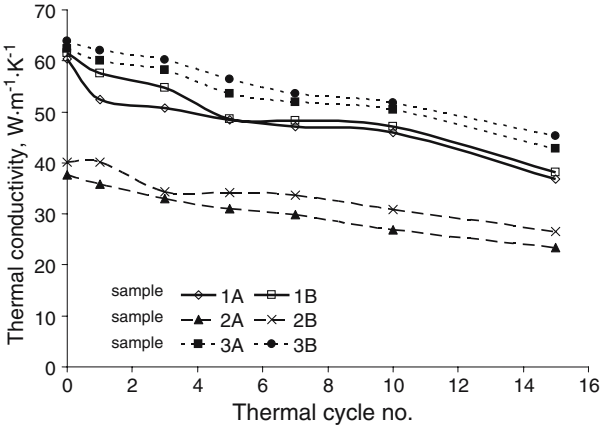

Fig. 4. Thermal conductivity of ceramic bars vs. thermal cycle number.

the model-fitting analysis were used for all measurements. The mass loss vs. cycle number is depicted in Fig. 5.

Figures 4 and 5 indicate that the thermal conductivity decreases in a manner similar to that of the decrease in sample mass and the degradation in mechanical strength after thermal cycling. The different thermal conductivity results at the A and B positions, shown in Fig. 4, are reproducible and indicate that the structural constitution in the ceramic bars is not homogeneous through the individual bars.

These results indicate that the THS technique, and possibly also the TPS technique, has a potential of being used as a non-destructive

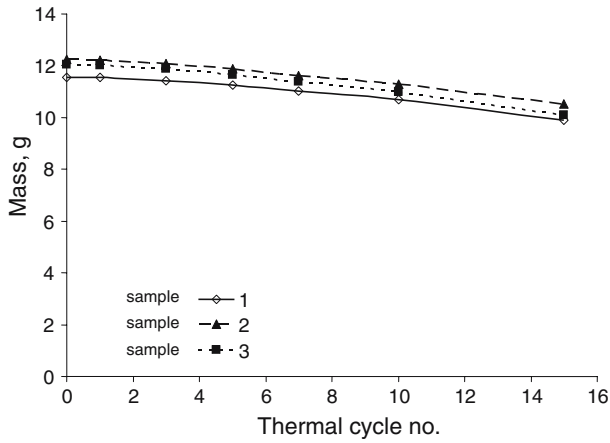

Fig. 5. Mass of ceramic bars vs. thermal cycle number.

evaluation technique for RCC materials using a single-sided measurement approach.

ACKNOWLEDGMENTS

This work is supported by the U.S. Department of Energy (DOE), Assistant Secretary for Energy Efficiency and Renewable Energy, Office of Transportation Technologies, as part of the High Temperature Materials Laboratory (HTML) User Program and Office of Industrial Technologies managed by the UT-Battelle LLC. for the DOE under Contract DE-AC05-000OR22725.

REFERENCES

1. S. E. Gustafsson, *Rev. Sci. Instrum.* **62**:797 (1991).
2. T. Log and S. E. Gustafsson, *Fire Mater.* **19**:43 (1995).
3. B. M. Suleiman, M. Gustavsson, E. Karawacki, and A. Lundén, *J. Phys. D: Appl. Phys.* **30**:2553 (1997).
4. M. Gustavsson, J. S. Gustavsson, S. E. Gustafsson, and L. Hälldahl, *High Temp.-High Press.* **32**:47 (2000).
5. D. Lundström, B. Karlsson, and M. Gustavsson, *Z. Metallkd.* **92**:1203 (2001).
6. Y. He, *Proc. 30th NATAS Conf.*, Pittsburgh, Pennsylvania (2002), pp. 499–504.
7. M. Gustavsson and S. E. Gustafsson, *Thermal Conductivity 26* (DEStech Pubs. Inc., Lancaster, Pennsylvania, 2001), pp. 367–377.
8. M. K. Gustavsson and S. E. Gustafsson, *Thermal Conductivity 27* (DEStech Pubs. Inc., Lancaster, Pennsylvania, 2003), pp. 338–346.
9. S. E. Gustafsson, E. Karawacki, and M. N. Khan, *J. Phys. D: Appl. Phys.* **12**:1411 (1979).

10. S. E. Gustafsson, M. A. Chohan, K. Ahmed, and A. Maqsood, *J. Appl. Phys.* **55**:3348 (1984).
11. S. E. Gustafsson, *Rigaku J.* **4**:16 (1987).
12. Y. W. Song, U. Groβ, and E. Hahne, *Fluid Phase Equilib.* **88**:291 (1993).
13. M. J. Lourenco, S. C. S. Rosa, C. A. Nieto de Castro, C. Albuquerque, B. Erdmann, J. Lang, and R. Roitzsch, *Int. J. Thermophys.* **21**:377 (2000).
14. S. E. Gustafsson, M. A. Chohan, and M. N. Khan, *High Temp. High Press.* **17**:35 (1985).
15. M. A. Chohan, *Pulse Transient Hot Strip Technique for Measurement of Thermal Properties of Non-Conducting Substances and Thin Insulating Layers on Substrates* Ph.D. thesis, (Dept. of Physics, Chalmers University of Technology, Sweden, 1987).
16. M. Gustavsson, H. Nagai, and T. Okutani, *Rev. Sci. Instrum.* **74**:4542 (2003).
17. M. Gustavsson, H. Nagai, and T. Okutani, *Int. J. Thermophys.* **26**:1803 (2005).
18. M. Gustavsson, E. Karawacki, and S. E. Gustafsson, *Rev. Sci. Instrum.* **65**:3856 (1994).
19. J. S. Gustavsson, M. Gustavsson, and S. E. Gustafsson, *Structural Mater. Technol. IV—An NDT Conf.* (2000), pp. 203–209.
20. T. Log and M. M. Metallinou, *Rev. Sci. Instrum.* **63**:3966 (1992).
21. G. Grimvall, "Thermophysical Properties of Materials" in *Selected Topics in Solid State Physics XVIII, ISBN 0-444-86985-9* (1986).
22. J. S. Gustavsson, M. Gustavsson, and S. E. Gustafsson, *Thermal Conductivity 24* (Technomic Pub. Co., Lancaster, Pennsylvania, 1997), pp. 116–122.
23. V. Bohac, M. Gustavsson, L. Kubicar, and S. E. Gustafsson, *Rev. Sci. Instrum.* **71**:2452 (2000).